Supporting Information for

Geometrical Re-organization of Dectin-1 and TLR2 on Single Phagosomes Alters Their Synergistic Immune Signaling

Wenqian Li[a,b], Jun Yan[c] and Yan Yu[a]

[a]Department of Chemistry, Indiana University, Bloomington, IN 47405-7102;

[b]Department of Molecular and Cellular Biochemistry, Indiana University, Bloomington, IN 47405-7003;

[c]Department of Medicine, School of Medicine, University of Louisville, Louisville, KY 40202.

This PDF file includes:

www.pnas.org/cgi/doi/10.1073/pnas.1909870116

Materials and Methods

Reagents and cells. 11-Mercaptoundecanoic acid (MUA) was purchased from Santa Cruz Biotechnology (Dallas, TX). 1,1'-Carbonyldiimidazole (CDI), 2-(N-morpholino)ethanesulfonic acid (MES), N-hydroxysuccinimide (NHS), bovine serum albumin (BSA), and IgG from rabbit serum were from Sigma-Aldrich (St. Louis, MO). Curdlan (β-1,3-glucan from *Alcaligenes faecalis*), Pam3CSK4 and rhodamine-labeled Pam3CSK4 were purchased from InvivoGen (San Diego, CA). Dimethyl sulfoxide (DMSO) and paraformaldehyde (PFA) were purchased from Avantor (Radnor, PA). Polytetrafluoroethylene (PTFE) ultrafree-CL centrifugal filter (0.45 μm pore size) was purchased from MilliporeSigma (St. Louis, MO). Phospho-Syk (Tyr525/526) monoclonal antibody (2710S) and Card9 antibody (12283S) were purchased from Cell Signaling Technology (Danvers, MA). Mouse/rat MyD88 antibody (AF3109) and human/mouse c-Rel antibody (AF2699) were purchased from R&D Systems (Minneapolis, MN). Aminated silica nanospheres (diameter: 500 nm and 1 μm) were purchased from nanoComposix (San Diego, CA). Aliphatic amine latex particles (diameter: 3 μm), 3-aminopropyltriethoxysilane (APTES), L-glutamine, 1-ethyl-3-(3-dimethylaminopropyl)carbodiimide (EDC), Alexa Fluor succinimidyl esters, Alexa Fluor 405 conjugated goat anti-rabbit antibody (A-31556), Alexa Fluor 568 conjugated rabbit anti-goat antibody (A-31556), Lipofectamine 3000 transfection reagent, Tumor necrosis factor (TNF) α mouse uncoated ELISA kit with plates (88-7324-86), 4',6-diamidino-2-phenylindole (DAPI), CellROX Deep Red, and Griess reagent kit were purchased from Thermo Fisher Scientific (Waltham, MA). Dulbecco's Modified Eagle's Medium (DMEM), penicillin-streptomycin and fetal bovine serum (FBS) were purchased from Corning (Corning, NY). Plasmids for MyD88 (Addgene #13092) and Card9 (Addgene #16253) were kindly provided by Prof. Ruslan Medzhitov at Yale University and Prof. William G. Kaelin at Harvard University, respectively. GFP-Dectin-1 expressing RAW264.7 macrophages were originally provided by Prof. David Underhill at Cedars-Sinai Medical Center. Cells were cultured in DMEM supplemented with 2 mM L-glutamine, 100 units/mL penicillin, 100 mg/mL streptomycin and 10% FBS.

Particle Fabrication and Characterization. To conjugate curdlan on particles, particles at a concentration of 1.3×10^9 particles/mL were rinsed and resuspended in anhydrous DMSO using 0.45 μm PTFE centrifugal filter. Because the density of particles is too similar to that of DMSO to sediment after centrifugation, filtration with 0.45 μm PTFE centrifugal filters was used in the cleaning step. Particles were mixed with 0.5 M CDI in anhydrous DMSO and the mixture was vortexed at room temperature for 1 h to activate the primary amine groups on particle surface. Afterwards, particles were rinsed and resuspended in DMSO containing 10 mg/mL curdlan. The mixture was vortexed at room temperature for 2 h. Finally, particles were rinsed with DMSO and then phosphate buffered saline (PBS). The resulted particles are referred to as uniform curdlan particles (uC).

To prepare bifunctional Janus curdlan-Pam3CSK4 particles (jCPam), particles conjugated with curdlan were resuspended in ethanol and dried on pre-cleaned glass microscope slides to form a particle monolayer via a convention evaporation process (1). The particle monolayer was coated sequentially with a 5 nm-thick film of chromium (Cr) and then a 50 nm-thick film of gold (Au) by using an Edwards Thermal Evaporator. After the deposition of metals, the particle monolayer was immersed overnight in 10 mM MUA in anhydrous ethanol and then rinsed with deionized water. To conjugate Pam3CSK4 on the gold-coated hemisphere of particles, the particle monolayer after thiolation was incubated with a

droplet of 0.1 M MES buffer (pH 6.0) containing 2.8 mM EDC and 6.9 mM NHS at room temperature for 30 min, rinsed with deionized water, and incubated with a droplet of 1× PBS buffer containing 30 μg/mL Pam3CSK4 at room temperature for 2 h. The volume of the droplets should be sufficient to cover the entire surface of the particle monolayer on microscope slides. After the reaction, the particle monolayer was rinsed in deionized water and harvested by sonication in 1× PBS buffer for further use. The morphology of the gold-coated Janus particles was characterized using scanning electron microscopy (SEM).

To fabricate uniform Pam3CSK4 particles (uP) and bifunctional uniform curdlan-Pam3CSK4 particles (uCPam), 3 μm latex particles and fabricated uniform curdlan particles were incubated with 30 μg/mL Pam3CSK4 in 1× PBS buffer at 4 ˚C overnight, rinsed and resuspended in 1× PBS buffer.

To fabricate the Janus curdlan-IgG particles (jCIgG), a monolayer of curdlan particles was first coated with thin layers of Cr and Au as described above. Fluorescence labeled IgG was then transferred onto the gold hemisphere of particles in the monolayer using a microcontact printing method described elsewhere (2). Uniform curdlan-IgG partiles (uCIgG) were prepared by incubating uniform curdlan particles (uC) with fluorescence labeled IgG (0.56 μg/mL in 1× PBS buffer). The presence of IgG on the particles was confirmed with fluorescence imaging. The fluorescence intensity of IgG on both the jCIgG and uCIgG particles was matched to be the same.

The surface density of curdlan on particles was estimated using the phenol-sulfuric acid method (3). Curdlan of known concentrations (from 0.1 to 1 mg/mL) in DMSO was mixed sequentially with 5 wt% phenol and sulfuric acid at a 1:1:100 volume ratio and incubated for 10 min. The absorbance at 490 nm of all the mixtures was measured and plotted as a function of curdlan concentration to obtain a calibration plot (Fig. S9). Particle samples containing unknown amount of curdlan were prepared and measured following the same procedure. The 490 nm absorbance measured from the particle sample was used to extrapolate the amount of curdlan from the calibration plot. Particle concentration was estimated using a hemocytometer. The surface density of curdlan was calculated as the total amount of curdlan divided by the number of particles. For estimating the surface density of Pam3CSK4 on particles, a Bradford protein assay was used following the standard procedure. Because the amine latex particles interfere with the Bradford assay, the amount of Pam3CSK4 remaining in supernatant after conjugation reaction with particles was measured and used to calculate the amount of Pam3CSK4 that was conjugated on particles.

To functionalize glass coverslips uniformly coated with curdlan and Pam3CSK4, clean coverslips were first aminated by incubating with 2% APTES in anhydrous ethanol solution at room temperature overnight. Aminated coverslips were then functionalized with curdlan and Pam3CSK4 following the same procedure described above.

Measurement of Phagocytosis Probability. GFP-Dectin-1 expressing RAW264.7 macrophages were plated at 1.8×10^5 cells per well in a 24-well plate in complete DMEM media overnight and subsequently stimulated with particles at an overall 5:1 particle-to-cell ratio for 1.5 h. Cells were rinsed with 1× PBS three times, detached from the plate using trypsin, and resuspended in 1× PBS buffer. The samples were analyzed using a BD LSR II flow cytometer. Forward scatter area (FSC-A), which indicates relative differences in cell size, and side scatter area (SSC-A), which indicates relative

differences in cell granularity, were collected. Cells with internalized particles were gated in FSC-SSC dot plots using software FlowJo and the percentage of cells with associated particles was quantified. The average number of internalized particles per cell was estimated from images acquired with differential interference contrast (DIC) microscopy.

Immunofluorescence Staining. GFP-Dectin-1 expressing RAW264.7 macrophages were plated on 35 mm glass coverslips overnight and serum starved for 5 h prior to imaging. Prior to fixation, coverslips with seeded cells were assembled into custom imaging chambers. After particles were added, the imaging chambers were briefly centrifuged (500 rcf, 30 s) to facilitate particle binding to cells and then incubated at 37 ˚C for varied periods of time as indicated. Cells were washed with ice-cold 1× PBS, fixed with 2% PFA on ice for 5 min, permeabilized with acetone at -20 ˚C for 5 min, blocked with 2% BSA at room temperature for 30 min, and stained sequentially with 2 μg/mL primary antibody at room temperature for 1 h and 2 μg/mL secondary antibodies at room temperature for 30 min. To prepare samples for total internal reflection fluorescence (TIRF) imaging of receptor clusters, cells were incubated on the curdlan-Pam3CSK4 coated or bare glass substrates for 35 min at 37 ˚C before fixation and immunostaining.

Fluorescence Imaging and Image Analysis. Confocal fluorescence images were acquired using a Leica TCS SP8 confocal microscope equipped with a Leica HC PL APO CS2 63×/1.20 TIRF objective, a Leica DFC9000 sCMOS camera and LAS X software. TIRF images were acquired using a Nikon Eclipse-Ti inverted microscope equipped with a 1.64 N.A. ×100 TIRF objective and an Andor iXon3 EMCCD camera. Super-resolution structured illumination microscopy (SIM) images were acquired using a DeltaVision OMX SR imaging system equipped with a Olympus Plan Apo 60×/1.42 PSF objective and a sCMOS camera. SIM images were processed using SoftWorx software and further image analysis was performed using ImageJ. The area of protein clusters in TIRF images were analyzed using the Analyze Particles plugin in ImageJ as described in previous paper (4). To analyze proximity between protein clusters in TIRF images, shifts between two imaging channels were corrected using affine transformation in ImageJ based on transformation calibration profiles generated with TetraSpeck particles. The x,y coordinates of individual cluster centroids were identified using a single-particle tracking algorithm reported previously (5). The nearest neighbor distance (NND) was calculated as the distance from the centroid of a cluster in the first channel to the closest centroid of a cluster in the second channel. Using the same procedure, we calculated the NND between two channels of TIRF images of the same TetraSpeck beads and used the calculated value as the inaccuracy of the NND measurement.

MyD88 and Card9 Transfection. GFP-Dectin-1 expressing RAW264.7 macrophages were seeded overnight to reach 60-70% confluency and switched to opti-MEM 2 h before transfection. Lipofectamine 3000 and DNA plasmids were mixed following manufacturer's instruction and added to cells. Cells in petri dishes were centrifuged at 300 rcf for 10 min before being placed in incubator for 5 h. Cells were then switched to DMEM for overnight incubation. DNA plasmid concentration was measured by absorbance at 260 nm using Nanodrop.

c-Rel Translocation Assay. GFP-Dectin-1 expressing RAW264.7 macrophages were seeded on glass coverslips overnight and serum starved for 5 h. Particles were added to cells at an overall 5:1 particle-to-cell ratio and incubated at 37 ˚C for 10 min. Cells were immunostained with human/mouse c-Rel

primary antibody and Alexa Fluor 568 conjugated rabbit-anti-goat secondary antibody following the same immunofluorescence staining procedure as described above. Nuclei of cells were counterstained with 300 nM DAPI for 5 min. Fluorescence images were acquired using a Leica TCS SP8 confocal microscope equipped with a Leica HC PL APO CS2 63×/1.20 TIRF objective, a Leica DFC9000 sCMOS camera and LAS X software. Twenty-five images were taken at different locations of each sample. Images were analyzed using ImageJ following a previously reported method (6). Briefly, a median filter (3 pixels in radius) was applied to remove noise and then automatic thresholding was used to generate a binary mask. For each pair of images, the nucleus mask was generated from the DAPI image and the cytoplasmic mask was generated by subtracting the DAPI mask from the c-Rel mask using image calculator (Fig. S7C). c-Rel fluorescence in nucleus and cytoplasm was separated by applying the nucleus and cytoplasmic masks to the original c-Rel fluorescence images. c-Rel fluorescence intensity per pixel was obtained and nuclear to cytoplasmic c-Rel fluorescence intensity ratios were calculated.

Measurement of TNFα Secretion. GFP-Dectin-1 expressing RAW264.7 macrophages were plated at 1.8×10^5 cells per well in a 24-well plate in complete DMEM for 5 h and then serum starved for another 5 h. Cells were stimulated with different types of particles for 24 h before the supernatants were collected. Particle concentration was varied to control the particle to cell ratio as specified in main text. TNFα level in the supernatants was measured using an ELISA kit according to manufacturer's instruction.

Measurement of Reactive Oxygen Species (ROS) Production. GFP-Dectin-1 expressing RAW264.7 macrophages were plated at 1×10^5 cells per well in a 96-well plate in complete DMEM media for 5 h and serum starved for 2 h. 5×10^5 particles and 5 μM CellROX Deep Red were added to stimulate and stain cells simultaneously. Samples were kept in an incubator for varied periods of time as indicated, before the fluorescence emission of CellROX Deep Red at Em 660 nm (Ex 630 nm) was measured using a BioTek multi-plate reader. Nitric oxide (NO) production was measured in cell supernatant by using the Griess assay following the manufacturer recommended protocol. 20 μL Griess reagent, 150 μL supernatant and 130 μL H_2O were added into 96-well plate and incubated for 30 min. Absorbance at 548 nm was measured with a BioTek multi-plate reader. NO concentrations in samples were calculated from calibration curve.

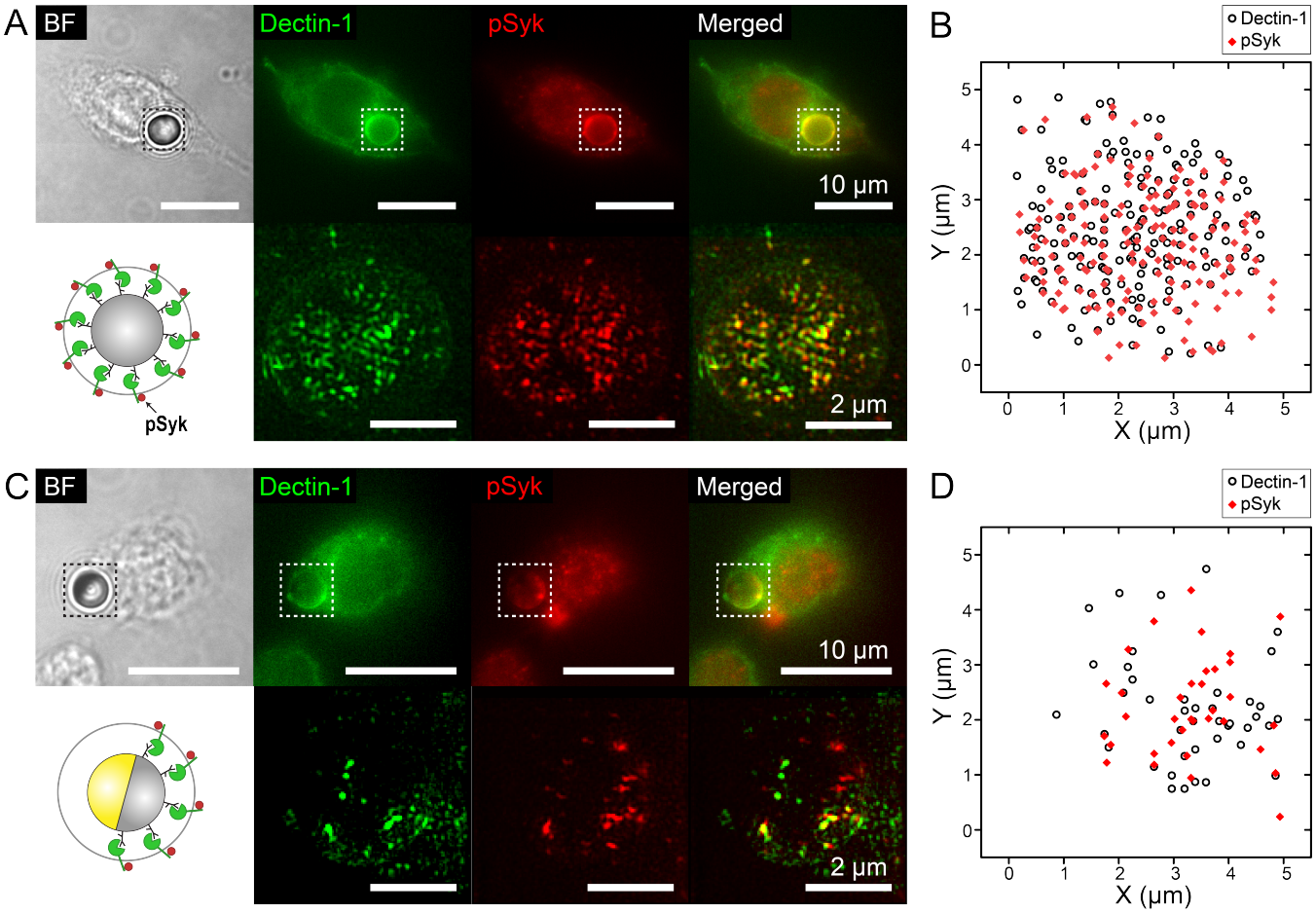

Fig. S1. Colocalization between Dectin-1 and pSyk nanoclusters confirms the activation of Dectin-1 receptors by curdlan on particles. (*A, C*) (*top*) Bright-field and SIM images showing Dectin-1 (green) and pSyk (red) fluorescence on the phagosome membranes encapsulating uniform curdlan particles (*A*) and Janus curdlan particles (*C*) (Scale bars: 10 μm). Zoomed-in images of the outlined areas are shown in the bottom row. (Scale bars for zoomed-in images: 2 μm). (*B, D*) Positions of Dectin-1 and pSyk nanoclusters as shown in zoomed-in images in (*A*) and (*C*) were identified using an object-based colocalization analysis. Each dot in the graphs represents the centroid position of a single protein cluster as indicated.

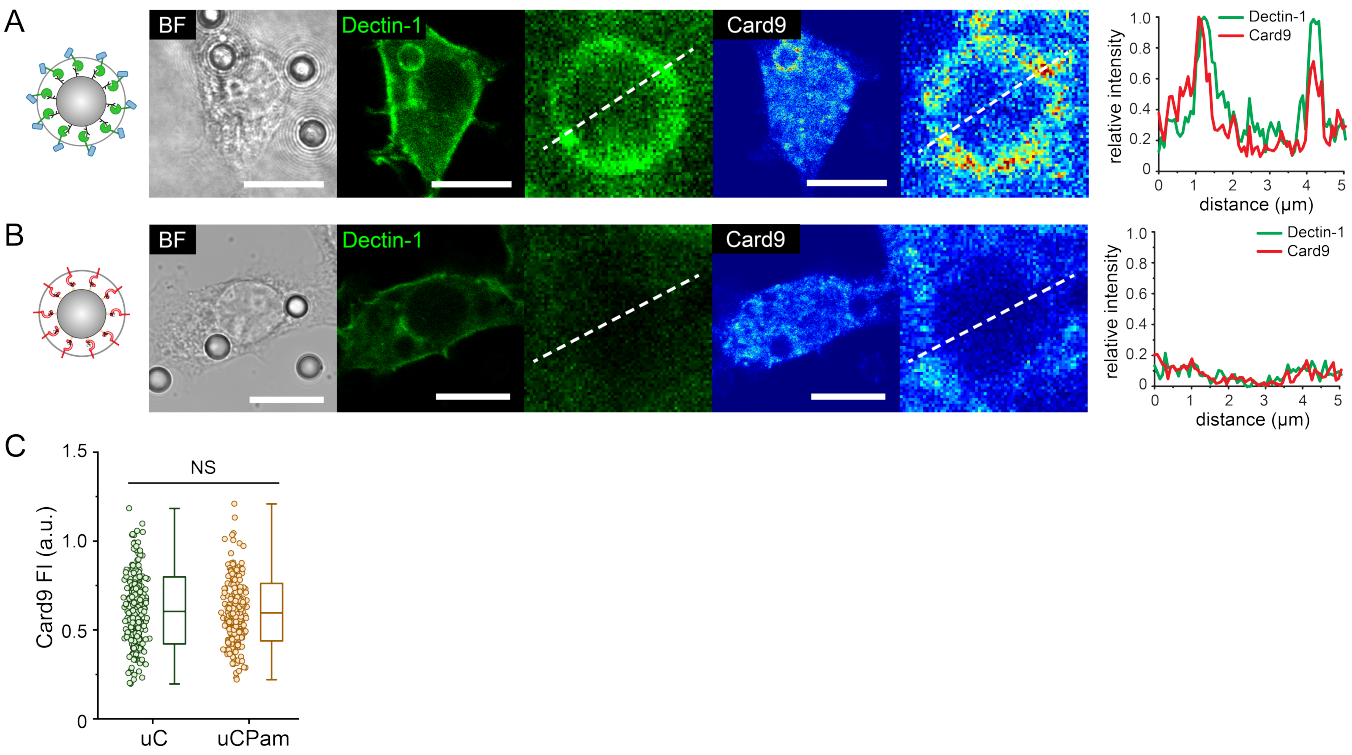

Fig. S2. Quantification of spatial distribution of Card9 on phagosomes. (*A, B*) Representative confocal images and line-scan plots showing Dectin-1(green) and Card9 (jet color) on phagosomes of uC particles (*A*) and uPam particles (*B*) (Scale bars: 10 μm). (*C*) Scatter plot showing fluorescence intensity of Card9 on phagosomes encapsulating uC particles and uCPam particles. Each point represents data from one phagosome, and data for each type of particle were obtained from ~250 cells in at least three independent experiments. Each box plot indicates the maximum to minimum, the median (horizontal line), and the standard deviation of the corresponding data set. Statistical significance is highlighted by *p*-values (Student's t test) as follows: NS not significant.

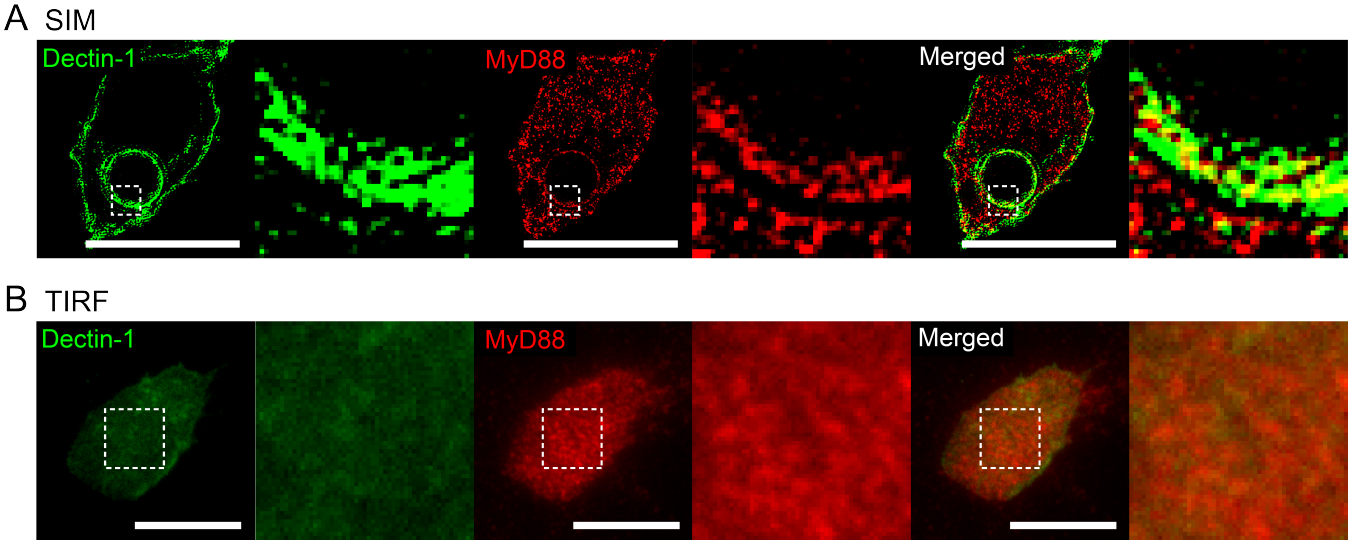

Fig. S3. (*A*) SIM images showing Dectin-1 and MyD88 nanoclusters on the membrane of a phagosome encapsulating a uniform curdlan-Pam3CSK4 particle (uCPam). (*B*) Representative TIRF images showing Dectin-1 and MyD88 nanoclusters in the cell membrane at the junction between RAW264.7 cells and a bare glass surface. Scale bars in all images: 10 μm.

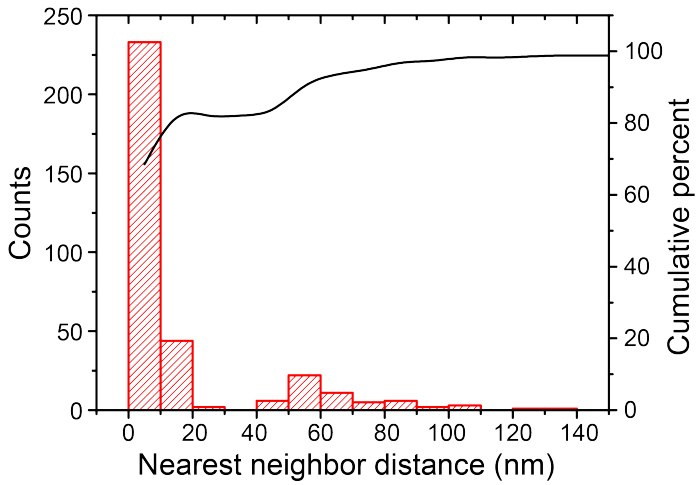

Fig. S4. Estimation of inaccuracy of nearest neighbor distance measurements. Histogram shows the distribution of NNDs measured from two emission channels of the same TetraSpeck particles.

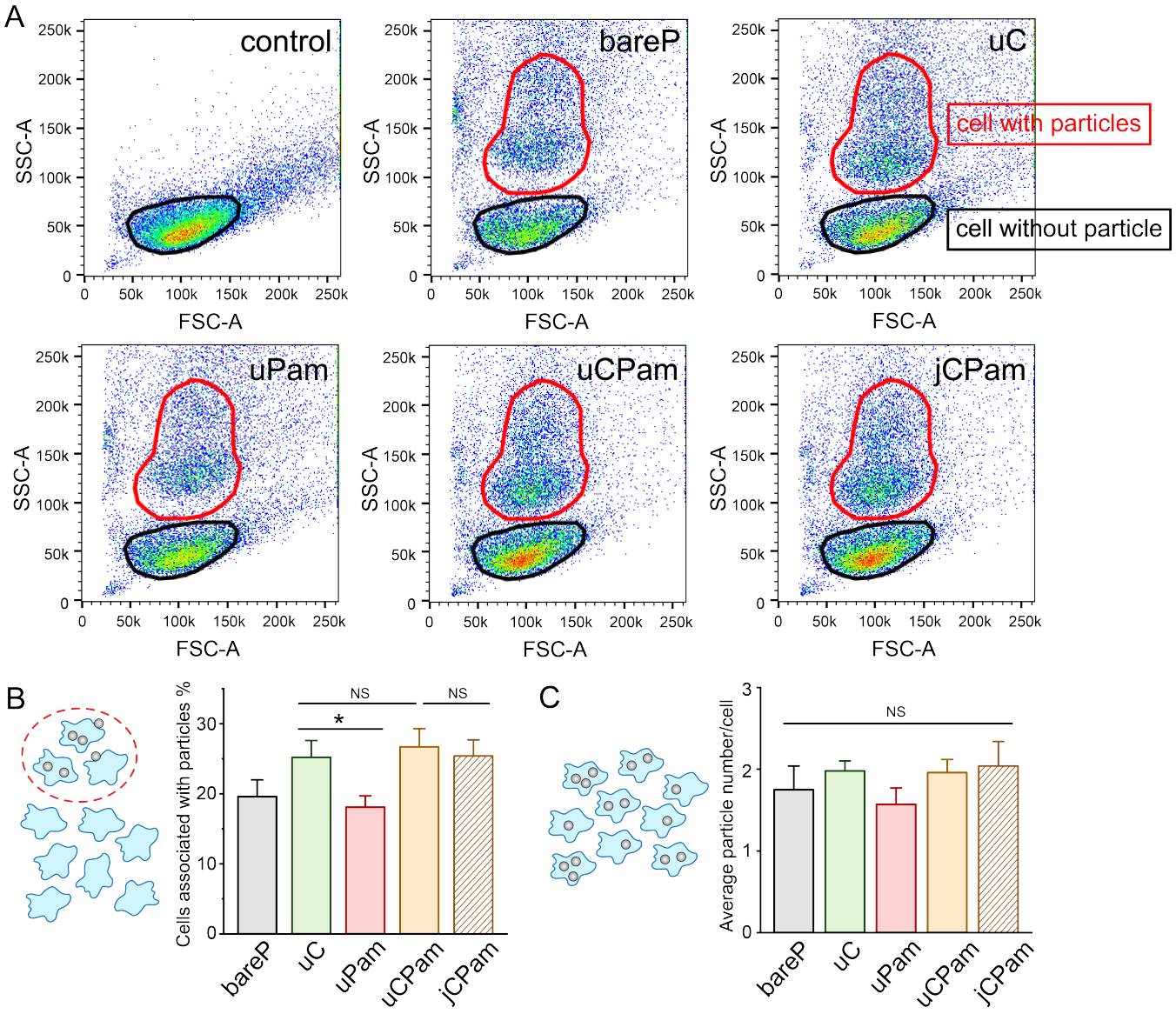

Fig. S5. Flow cytometry measurement of macrophage phagocytosis of particles. (*A*) Dot plots show forward scatter-area (FSC-A) versus side scatter-area (SSC-A) for macrophages stimulated with particles and two gates were created by FlowJo to stand for cells with particles and cells without particle. (*B*) Bar graph showing the percentage of cells containing internalized or surface-bound particles after 1.5 h stimulation by different types of particles. (*C*) Bar graph showing average number of internalized particles per cell obtained from differential interference contrast images after 24 h incubation. Each data bar represents the mean and standard error obtained from three independent experiments each performed in triplicate. Statistical significance is highlighted by *p*-values (Student's t test) as follows: * $p < 0.05$, NS not significant.

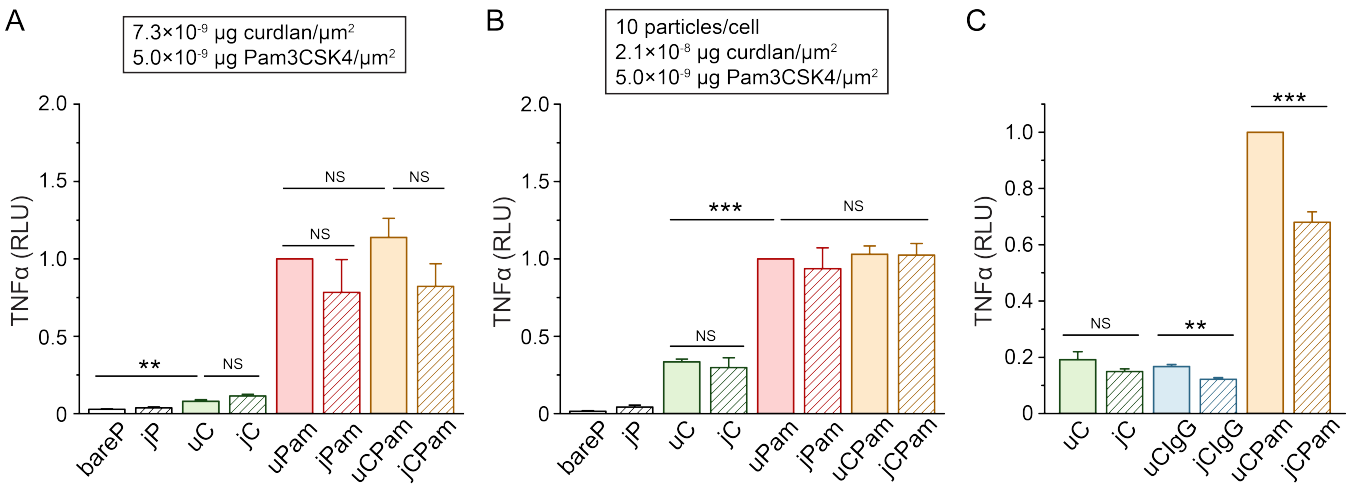

Fig. S6. Measurements of TNFα secretion in RAW264.7 macrophages upon stimulation by particles with different ligand densities (*A*), particle-to-cell ratios (*B*) and different ligand types (*C*). The average particle-to-cell ratio was 5:1 in (*A, C*) and 10:1 in (*B*). In all plots, each data bar represents the mean and standard error obtained from three independent experiments each performed in triplicate. All measurements were normalized to data from cells stimulated by uCPam particles. Statistical significance is highlighted by *p*-values (Student's t test) as follows: *** $p < 0.001$, ** $p < 0.01$, NS not significant.

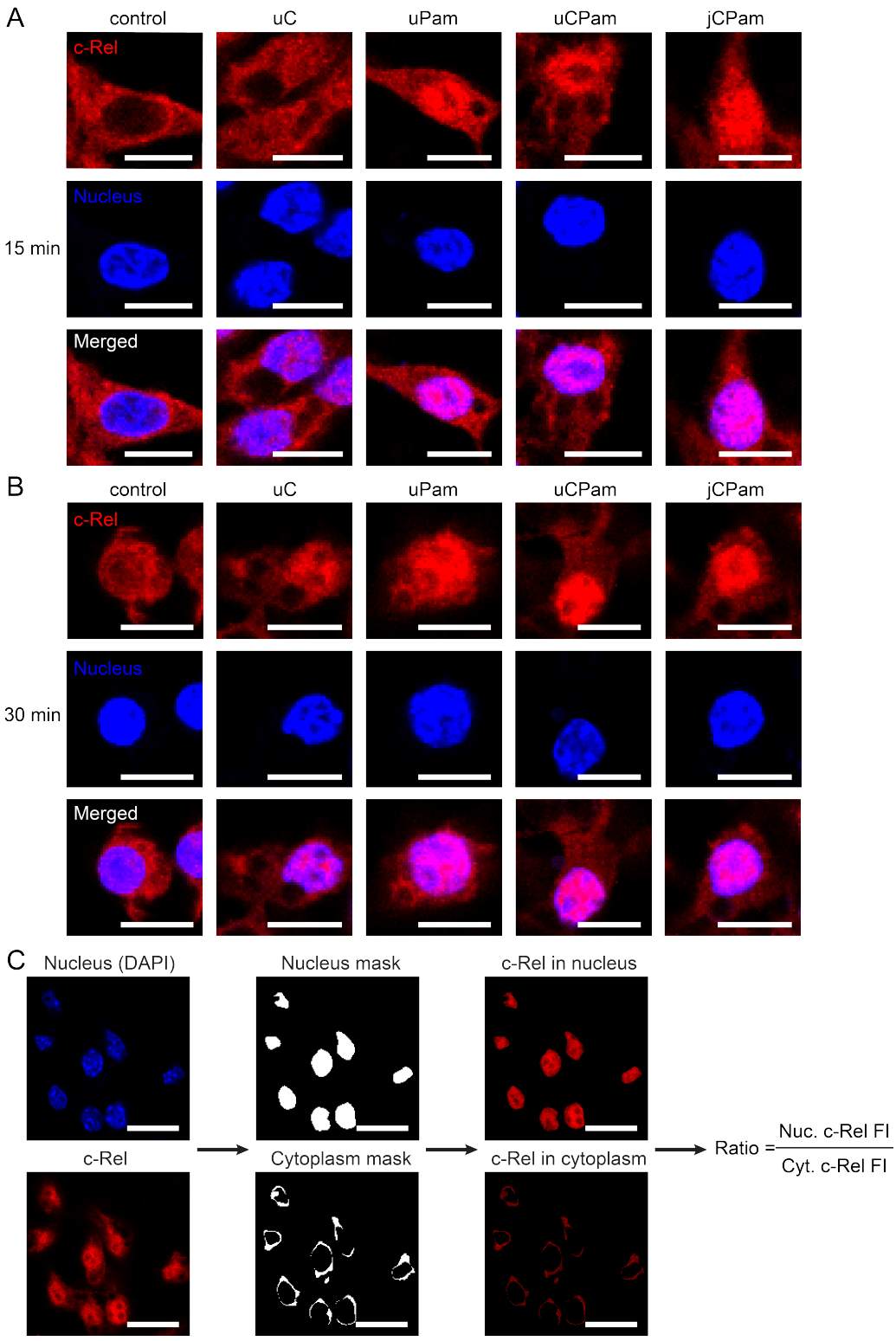

Fig. S7. Characterization of c-Rel translocation. (*A*, *B*) Representative immunofluorescence images showing c-Rel (red), nucleus (blue), and overlay in RAW264.7 macrophages. Macrophages were untreated (control) or stimulated with different types of particles for 15 min (*A*) or 30 min (*B*). Antibodies and DAPI were used to label c-Rel and nucleus, respectively. (Scale bars: 10 μm) (*C*) Flow

chart illustrating the quantification of c-Rel nucleus-to-cytoplasm ratio. Each set of fluorescence images (*left column*) of nucleus (blue) and c-Rel (red) was used to obtain binary masks (*middle column*), which were then applied to images of c-Rel to obtain fluorescence intensity of c-Rel in the nucleus and the cytoplasm (*right column*). (Scale bars: 20 μm)

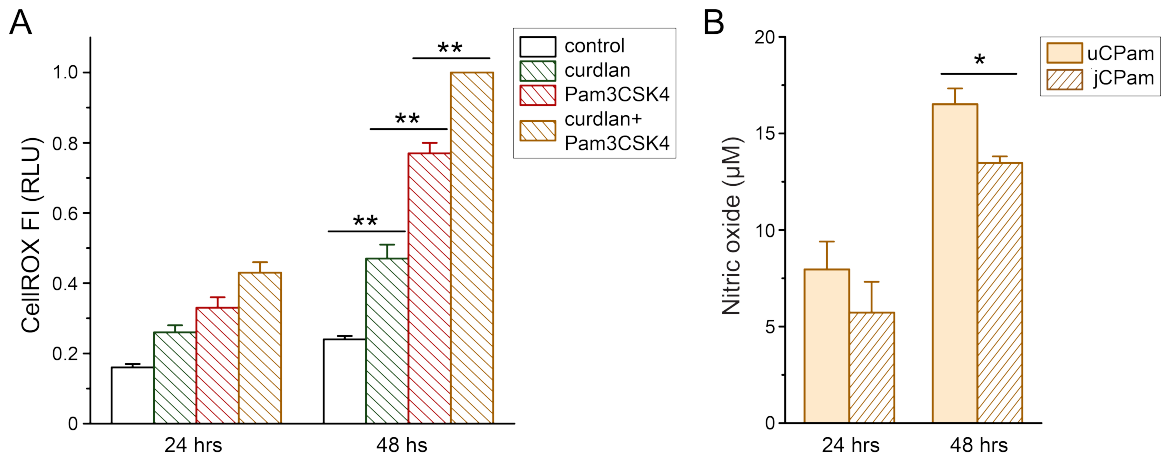

Fig. S8. (*A*) Measurement of ROS production in RAW264.7 macrophages upon stimulation by free ligands free ligands and stained after 24 h and 48 h. (*B*) Nitric oxide production of RAW264.7 macrophages upon stimulation by different types of particles. Each data bar represents the mean and standard error obtained from three independent experiments each performed in triplicate. Statistical significance is highlighted by *p*-values (Student's t test) as follows: **p < 0.01, *p < 0.05.

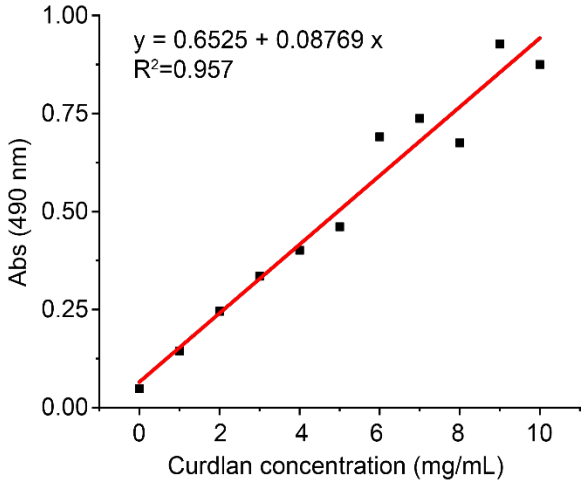

Fig. S9. Calibration curve for measuring curdlan concentration.

References

1. Y. Gao, Y. Yu, How half-coated janus particles enter cells. *J. Am. Chem. Soc.* **135**, 19091-19094 (2013).
2. Y. Gao, Y. Yu, Macrophage uptake of Janus particles depends upon Janus balance. *Langmuir* **31**, 2833-2838 (2015).
3. M. Dubois, G. K. A., J. K. Hamilton, P. A. Rebers, F. Smith, Colorimetric method for determination of sugars and related substances. *Anal. Chem.* **28**, 350-356 (1956).
4. F. B. Lopes *et al.*, Membrane nanoclusters of FcγRI segregate from inhibitory SIRPα upon activation of human macrophages. *J. Cell. Biol.* **216**, 1123-1141 (2017).
5. R. Parthasarathy, Rapid, accurate particle tracking by calculation of radial symmetry centers. *Nat. Methods* **9**, 724-726 (2012).
6. M. Noursadeghi *et al.*, Quantitative imaging assay for NF-κB nuclear translocation in primary human macrophages. *J. Immunol. Methods* **329**, 194-200 (2008).